

# Quantification of the Effects of Organic and Carbonate Buffers on Arsenate and Phosphate Adsorption on a Goethite-Based Granular Porous Adsorbent

MASAKAZU KANEMATSU,<sup>\*,†</sup>  
 THOMAS M. YOUNG,<sup>†</sup>  
 KEISUKE FUKUSHI,<sup>‡</sup>  
 DIMITRI A. SVERJENSKY,<sup>§</sup>  
 PETER G. GREEN,<sup>†</sup> AND  
 JEANNIE L. DARBY<sup>†</sup>

*Department of Civil and Environmental Engineering, University of California—Davis, One Shields Avenue, Davis, California 95616, United States of America; Institute of Nature and Environmental Technology, Kanazawa University, Kakuma, Kanazawa, Ishikawa 920-1192, Japan; and Department of Earth and Planetary Sciences, The Johns Hopkins University, Baltimore, Maryland 21218, United States of America*

Received August 5, 2010. Revised manuscript received November 9, 2010. Accepted November 11, 2010.

Interest in the development of oxide-based materials for arsenate removal has led to a variety of experimental methods and conditions for determining arsenate adsorption isotherms, which hinders comparative evaluation of their adsorptive capacities. Here, we systematically investigate the effects of buffer (HEPES or carbonate), adsorbent dose, and solution pH on arsenate and phosphate adsorption isotherms for a previously well characterized goethite-based adsorbent (Bayoxide E33 (E33)). All adsorption isotherms obtained at different adsorbate/adsorbent concentrations were identical when 1 mM of HEPES (96 mg C/L) was used as a buffer. At low aqueous arsenate and phosphate concentration ( $\sim 1.3 \mu\text{M}$ ), however, adsorption isotherms obtained using 10 mM of  $\text{NaHCO}_3$  buffer, which is a reasonable carbonate concentration in groundwater, are significantly different from those obtained without buffer or with HEPES. The carbonate competitive effects were analyzed using the extended triple layer model (ETLM) with the adsorption equilibrium constant of carbonate calibrated using independent published carbonate adsorption data for pure goethite taking into consideration the different surface properties. The successful ETLM calculations of arsenate adsorption isotherms for E33 under various conditions allowed quantitative comparison of the arsenate adsorption capacity between E33 and other major adsorbents initially tested under varied experimental conditions in the literature.

\* Corresponding author phone: 530-400-5375; e-mail: mkanematsu@ucdavis.edu.

<sup>†</sup> Department of Civil and Environmental Engineering, University of California—Davis.

<sup>‡</sup> Institute of Nature and Environmental Technology, Kanazawa University.

<sup>§</sup> Department of Earth and Planetary Sciences, The Johns Hopkins University.

## Introduction

Arsenic (As) occurs naturally in groundwaters across the world and has been a serious threat to human health (1). Because of human health concerns, the maximum contaminant level (MCL) for arsenic in potable water was reduced to  $10 \mu\text{g/L}$  as As in the U.S. (2). For small water systems adsorption has been recognized as one of the most suitable arsenic removal technologies, and many nanostructured metal oxide-based adsorbents for arsenic removal have been developed (3). Arsenic is commonly found in two major oxidation states: arsenate (As(V)) and arsenite (As(III)). Arsenate is more strongly adsorbed onto metal oxides than arsenite (4), therefore arsenite is typically oxidized to arsenate prior to adsorption in water treatment systems.

Research aimed at developing and demonstrating nanostructured metal oxide-based adsorbents for arsenate removal has focused on the determination of arsenate adsorption isotherms for these adsorbents (5–10). Generally, a single adsorption isotherm is measured to provide initial information about the feasibility of using a particular adsorbent in a particular application, to compare the capacity of one adsorbent to others, and to design adsorption treatment systems such as fixed-bed adsorbers (11). Adsorption isotherms are typically obtained using batch reactors prepared in two different ways (11): In Method 1 (constant dose) the same quantity of adsorbent is added to solutions with different initial solute concentrations (5, 6, 12); in Method 2 (variable dose) different quantities of adsorbent are added to solutions with the same initial solute concentration (7–9). It is possible that the two methods produce different adsorption isotherms, especially when competing species are used as pH buffers. Typically arsenate adsorption isotherm studies are conducted experimentally at a pH value fixed by an organic or inorganic buffer (5–10) because of the reasons stated below. Moreover, initial arsenate concentrations are often extremely high when Method 1 is used (6). This may lead to the possibility of arsenate precipitation which could result in overestimation of arsenate removal capacity using fitted adsorption isotherms. Hence, systematic surface chemistry studies of arsenate adsorption on such oxide materials should be carried out over a wide range of conditions, such as a range of pH values, the presence or absence of buffers, and a range of adsorbate to solid loading ratios.

Because arsenate adsorption on metal oxide is strongly pH dependent, it is critical to maintain a constant pH during adsorption isotherm tests. Arsenate adsorption isotherms on pure metal oxides are generally determined without buffers, and solution pH is maintained by adding small amounts of acid and/or base as needed (4, 13) for two reasons. First, adsorption reactions on mineral surfaces are very fast (less than 24 h) so that it is relatively easy to keep pH constant during adsorption tests. Second, adding another component into the systems is undesirable because it may compete with the target component. In the case of nanostructured porous metal oxide adsorbents, arsenate adsorption isotherm experiments are often conducted by adding organic buffers (e.g., HEPES (5) and BES 6, 14) or sodium bicarbonate ( $\text{NaHCO}_3$ ) (8, 9, 14). Because arsenate surface diffusion into the pores is slow and rate-limiting (8, 12), it takes longer to reach adsorption equilibrium in porous metal oxide-based adsorbent-water systems. Previous studies have not indicated that those buffers will affect arsenate adsorption (15, 16).

The effects of carbonate and organic species adsorption in the presence of arsenate and phosphate have been reported

for pure mineral systems. Stachowicz et al. (17) stated that carbonate may compete with both arsenate and arsenite adsorption, while Rahnamaie et al. (18) concluded that carbonate species bind much more weakly than phosphate onto goethite. Arai et al. (19) concluded that the effects of dissolved carbonate on arsenate adsorption are influenced by reaction conditions such as available surface sites, initial arsenate concentrations, and reaction times. In their experiments (19), different adsorbed carbonate concentrations, associated with two different atmospheric compositions, resulted in an enhanced and/or suppressed arsenate adsorption. Although adsorption of organic buffers on metal oxides has not been studied thoroughly, binding of organic acids on metal oxides is relatively weak (16). Therefore, it is still unclear how these species affect measured arsenate adsorption isotherms, especially for commercial nanostructured granular porous adsorbents and for conditions when aqueous concentrations of arsenate are as low as the MCL (i.e., 10 µg/L as As).

Recently, the characteristics of arsenate and phosphate adsorption on a well-characterized commercial nanostructured granular porous goethite-based adsorbent known as Bayoxide E33 (E33) were established over a wide range of pH values, surface loading and ionic strengths (12). This adsorbent is one of the most frequently used for arsenic removal in small water systems, and it rated as the best performing adsorbent in pilot studies (3). Here, we extend the results of our recent study by determining arsenate and phosphate adsorption isotherms on E33 under various conditions and by examining the effects of buffers (HEPES or NaHCO<sub>3</sub>) on adsorption. We applied the extended triple layer surface complexation model (ETLM) to these data using protonation and electrolyte adsorption constants determined in our previous study. In order to do this, we also developed a surface complexation model for carbonate calibrated on published adsorption data for a pure goethite.

The specific objectives of this work were (1) to understand how different experimental methods such as choice of buffers (e.g., no buffer, HEPES, and NaHCO<sub>3</sub>), adsorbate/adsorbent concentrations, and solution pH affect arsenate and phosphate adsorption isotherms of E33; (2) to predict arsenate and phosphate adsorption isotherms under various conditions including carbonate competitive effects using the ETLM approach; and (3) to quantitatively compare the arsenate adsorption capacity of E33 with other major adsorbents reported in the literature to illustrate the utility of surface complexation models in making such comparisons.

## Materials and Methods

**Materials.** Arsenate and phosphate stock solutions were prepared from reagent grade Na<sub>2</sub>HAsO<sub>4</sub>·7H<sub>2</sub>O and NaH<sub>2</sub>PO<sub>4</sub>·H<sub>2</sub>O (Sigma Aldrich, St. Louis, MO), respectively. Reagent grade sodium bicarbonate and HEPES sodium salt (Fisher Scientific, Pittsburgh, PA) were used as buffers. The dry-granular goethite-based porous adsorbent, E33, was crushed, washed, and wet-sieved using a 200 × 325 U.S. standard mesh sieve to shorten experimental time to reach equilibrium. The washed E33 was dried in an oven at 40 °C for two days to avoid any phase modification or transformation (20), and then stored in a desiccator. Dried E33 was suspended in deionized water for at least two days prior to all experiments. The BET surface area and p*H*<sub>zpc</sub> of E33 are 158.1 m<sup>2</sup>/g and 8.5, respectively (12, 21). Detailed description of the adsorbent is available elsewhere (12, 21).

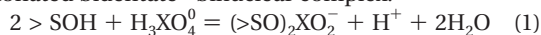
**Adsorption Isotherms.** Arsenate and phosphate adsorption isotherms were determined using the two approaches described above. In Method 1, the adsorbent dosage was fixed at 0.025 g/L. Duplicates of 800 mL solutions having a fixed amount of E33 (20 mg) and different initial solute concentrations were prepared in 1000 mL plastic bottles.

This experiment was conducted without buffer at pH 7.0 (a constant pH was carefully maintained by adding HNO<sub>3</sub> and NaOH), with 10 mM of NaHCO<sub>3</sub> at pH 7.0 and 8.3, and with 1 mM of HEPES at pH 7.0. Without buffer, pH had to be adjusted frequently during the first three days. In Method 2, duplicates of 4000 mL solutions having different amounts of solid (10–160 mg) and fixed initial solute concentrations (120 µg/L as As or P) were prepared in 4 L plastic bottles. This experiment was conducted with 10 mM of NaHCO<sub>3</sub> at pH 7.0 and 8.3, and with 1 mM of HEPES at pH 7.0. Ionic strength was adjusted to 0.02 M using NaNO<sub>3</sub>, and pH was carefully monitored and adjusted to the target pH values ±0.1 during the experiments, if necessary. All bottles were tumbled for seven days to reach adsorption equilibrium.

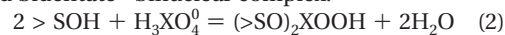
The pH was measured with a glass electrode and a pH meter (Mettler Toledo, Columbus, OH). Arsenate concentrations were analyzed using inductively coupled plasma-mass spectrometry (Agilent Technologies, Wilmington, DE). Phosphate concentrations were analyzed by a colorimetric method using a flow injection analyzer (FIA) (Lachat Instruments, Milwaukee, WI). A detailed description of the batch adsorption experiments can be found elsewhere (12).

**Extended Triple Layer Modeling.** The ETLM is a surface complexation model integrated with spectroscopic and molecular evidence (22). Recently, adsorption of many ions including arsenate (23) on many oxides have been systematically modeled by the ETLM. In our previous study, adsorption equilibrium constants of arsenate and phosphate were determined for E33 in the absence of buffers. In this study, all ETLM calculations were performed using the computer code GEOSURF (24). Aqueous ionic activity coefficients of dissolved species were calculated with the extended Debye–Hückel equation. The surface complexation reactions of arsenate and phosphate are described in eq 1–6 (12), although there is ongoing discussion regarding the precise nature of the surface complexes formed (25, 26). The electrostatic terms for the surface complexation reactions of arsenate and phosphate are described in eq 7–9. The relationships of the site-occupancy standard states to the hypothetical 1.0 M standard states for the arsenate and phosphate surface species are described in eqs 10–12.

deprotonated bidentate–binuclear complex:



protonated bidentate–binuclear complex:



monodentate complex:



$$*K_{>\text{SO})_2\text{XO}_2^-}^\theta = \frac{a_{(>\text{SO})_2\text{XO}_2^-} a_{\text{H}^+} a_{\text{H}_2\text{O}}^2}{a_{>\text{SOH}}^2 a_{\text{H}_3\text{XO}_4^0}} 10^{F(\Delta\Psi_{r,1})/2.303RT} \quad (4)$$

$$*K_{(>\text{SO})_2\text{XOOH}}^\theta = \frac{a_{(>\text{SO})_2\text{XOOH}} a_{\text{H}_2\text{O}}^2}{a_{>\text{SOH}}^2 a_{\text{H}_3\text{XO}_4^0}} 10^{F(\Delta\Psi_{r,2})/2.303RT} \quad (5)$$

$$*K_{>\text{SOXO}_3^{2-}}^\theta = \frac{a_{>\text{SOXO}_3^{2-}} a_{\text{H}^+}^2 a_{\text{H}_2\text{O}}}{a_{>\text{SOH}} a_{\text{H}_3\text{XO}_4^0}} 10^{F(\Delta\Psi_{r,3})/2.303RT} \quad (6)$$

$$\Delta\psi_{r,1} = 2\psi_0 - 3\psi_\beta - 2(\psi_0 - \psi_\beta) = -\psi_\beta \quad (7)$$

$$\Delta\psi_{r,2} = 2\psi_0 - 2\psi_\beta - 2(\psi_0 - \psi_\beta) = 0 \quad (8)$$

$$\Delta\psi_{r,3} = \psi_0 - 3\psi_\beta - (\psi_0 - \psi_\beta) = -2\psi_\beta \quad (9)$$

$$\log *K_{(>SO)_2XO_2}^{\theta} = \log *K_{(>SO)_2XO_2}^{\theta} + \log \left( \frac{(N_s A_s)^2}{N^{\ddagger} A^{\ddagger}} C_s \right) \quad (10)$$

$$\log *K_{(>SO)_2XOOH}^{\theta} = \log *K_{(>SO)_2XOOH}^{\theta} + \log \left( \frac{(N_s A_s)^2}{N^{\ddagger} A^{\ddagger}} C_s \right) \quad (11)$$

$$\log *K_{>SOXO_3^-}^{\theta} = \log *K_{>SOXO_3^-}^{\theta} + \log \left( \frac{N_s A_s}{N^{\ddagger} A^{\ddagger}} \right) \quad (12)$$

Here, X stands for As(V) or P.  $*K_i^{\theta}$  represents the adsorption equilibrium constant for the formation of surface species  $i$ , and the superscript " $\theta$ " represents the site-occupancy standard state (27, 28). Adsorption equilibrium constants are represented relative to the surface species  $>SOH$ , and this is indicated by the superscript " $\theta$ ". The exponential terms correct for activity differences of ions from the bulk solution caused by the surface potential field ( $\Delta\psi_r$ ), where  $F$ ,  $R$ , and  $T$  represent Faraday's constant (96,485 [C·m<sup>-2</sup>]), the gas constant (8.314 J mol<sup>-1</sup> K<sup>-1</sup>), and absolute temperature [K], respectively.  $N_s$  represents the surface site density on the  $s$ th solid sorbent (site/nm<sup>2</sup>);  $N^{\ddagger}$  represents the standard state adsorbate species site density (sites/m<sup>2</sup>);  $A_s$  represents the BET surface area of the  $s$ th solid adsorbent (m<sup>2</sup>/g);  $C_s$  is the solid concentration (g/L);  $A^{\ddagger}$  represents the standard state BET surface area (m<sup>2</sup>/g). In this study, values of  $N^{\ddagger} = 10$  (site/nm<sup>2</sup>) and  $A^{\ddagger} = 10$  (m<sup>2</sup>/g) are selected for solids (28).

Carbonate surface complexes have been examined by in situ attenuated total reflectance-Fourier transform infrared (ATR-FTIR) spectroscopy on goethite (29–31) and hematite (32, 33). All of the studies except Bargar et al. (2005) (33) assigned carbonate surface complex structures to monodentate–mononuclear inner-sphere species. Bargar (33) assigned their experimental IR spectra to density functional theory (DFT)/molecular orbital (MO)-calculated frequencies and suggested that two carbonate species exist on hematite, one an inner-sphere bidentate binuclear surface complex and the other an outer-sphere or hydrogen bonded carbonate complex. The outer-sphere or hydrogen bonded species was only observed in the absence of ionic strength control. They ruled out the possibility of any monodentate-mononuclear species because none of the calculated vibration frequencies for these species were able to reproduce the experimental IR spectra.

Villalobos and Leckie (34) conducted carbonate adsorption experiments on goethite under a wide range of pH, ionic strength, and surface coverage values under both open and closed system conditions. Villalobos and Leckie (30) describe their adsorption data using a modified TLM. They obtained a reasonable model fit by assuming that carbonate adsorbs as a monodentate mononuclear species  $>SOCOO^-$ , with a charge allocation of 0 and  $-1$  on the  $\alpha$ - and  $\beta$ -planes, respectively. Improved model fits were achieved by a charge allocation of 0.2 and 0.8 on the  $\alpha$ - and  $\beta$ -planes, respectively with protonated monodentate species ( $>SOCOOH$ ) and Naternary species ( $>SOCOONa$ ). Hiemstra et al. (35) analyzed the same carbonate adsorption data with a CD-MUSIC model, and they showed that a bidentate binuclear species ( $>(SO)_2CO$ ) could fit the adsorption data. Rahnemaie et al. (18) also concluded that the bidentate inner-sphere complex ( $>(SO)_2CO$ ) is dominant.

In our present study, the carbonate adsorption data on goethite provided by Villalobos and Leckie (34) was analyzed using the ETLM. Basic surface parameters including the surface protonation constants, the electrolyte adsorption constants and the inner-layer capacitance were taken from refs 27 and 28 (Table S1 of the Supporting Information). The site density for the goethite was determined as a fitting parameter in the ETLM for carbonate adsorption data as a

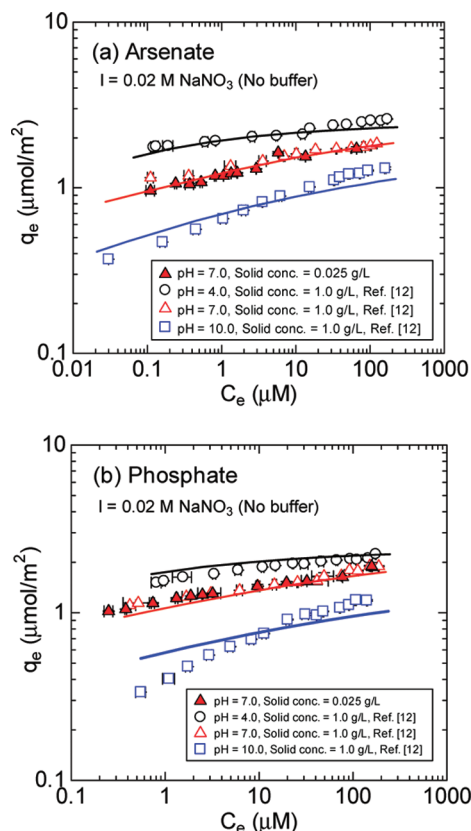
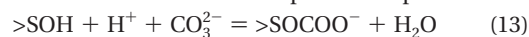


**FIGURE 1.** Arsenate (a) and phosphate (b) adsorption isotherms for E33 in 0.02 M NaNO<sub>3</sub> solution without buffers shown together with the ETLM predictions (solid lines). The correlation coefficients ( $R^2$ ) of the ETLM predictions for arsenate (Figure 1a) at pH 4, 7, and 10 are 0.99, 0.99, and 0.98, respectively. Those for phosphate (Figure 1b) at pH 4, 7, and 10 are 0.98, 0.98, and 0.96 (pH 10), respectively.

function of surface coverage because the site density of goethite varies depending on the type of goethite (23). In the ETLM analyses for carbonate adsorption on goethite, a single reaction involving a deprotonated monodentate mononuclear inner sphere species ( $>SOCOO^-$ ) can describe all of the experimental data as shown below. The surface complexation reaction, the corresponding mass law expression, and the description of  $\Delta\psi_r$  are given by eq 13–15.

Monodentate-mononuclear inner-sphere complex:



$$*K_{>SOCOO^-}^{\theta} = \frac{a_{>SOCOO^-} a_{H_2O}}{a_{>SOH} a_{H^+} a_{CO_3^{2-}}} 10^{F(\Delta\psi_r)/2.303RT} \quad (14)$$

$$\Delta\psi_r = \psi_0 - 2\psi_{\beta} - 1(\psi_0 - \psi_{\beta}) = -\psi_{\beta} \quad (15)$$

Most of the infrared information indicates that there is a single dominant inner-sphere surface species in the presence of background electrolyte ions under a wide range of pH conditions. Most infrared studies indicate that the inner-sphere species is a deprotonated species. These spectroscopic observations are consistent with the present ETLM of carbonate adsorption. Interestingly, the obtained  $\Delta\psi_r$  (eq 15) is the same as that of the charge allocation employed in the modified TLM (30), suggesting that the unusual charge allocation in the TLM proposed by Villalobos and Leckie (30) could be explained by including the electrostatic work of desorption of the water dipole from the goethite surface during anion adsorption by ligand

**TABLE 1. Characteristics and the Extended Triple Layer Model (ETLM) Parameters of Bayoxide E33 (Surface Protonation Constants, Electrolyte Adsorption Constants, and Adsorption Equilibrium Constants of Arsenate, Phosphate, and Carbonate)**

name	reaction	log <i>K</i>
Hypothetical 1.0 M Standard State		
log $K_1^0$	$>SOH + H^+ = >SOH_2^+$	4.9
log $K_2^0$	$>SO^- + H^+ = >SOH$	-12.1
log $*K_{Na^+}^0$	$>SOH + Na^+ = >SO^- Na^+ + H^+$	-8.7
log $*K_{NO_3^-}^0$	$>SOH + H^+ + NO_3^- = >SOH_2^+ NO_3^-$	8.0
Site-Occupancy Standard State		
log $K_{(>SO)_2AsO_2^-}^0$	$2 > SOH + H_3AsO_4^0 = (>SO)_2AsO_2^- + H^+ + 2H_2O$	2.9
log $K_{(>SO)_2AsOOH}^0$	$2 > SOH + H_3AsO_4^0 = (>SO)_2AsOOH + 2H_2O$	2.4
log $K_{>SOAsO_4^{3-}}^0$	$>SOH + H_3AsO_4^0 = >SOAsO_3^{2-} + 2H^+ + H_2O$	-0.2
log $K_{(>SO)_2PO_2^-}^0$	$2 > SOH + H_3PO_4^0 = (>SO)_2PO_2^- + H^+ + 2H_2O$	2.3
log $K_{(>SO)_2POOH}^0$	$2 > SOH + H_3PO_4^0 = (>SO)_2POOH + 2H_2O$	1.6
log $K_{>SOPo_4^{3-}}^0$	$>SOH + H_3PO_4^0 = >SOPo_3^{2-} + 2H^+ + H_2O$	-0.1
log $K_{>SOCOO^-}^0$	$>SOH + H^+ + CO_3^{2-} = >SOCOO^- + H_2O$	-6.9

<sup>a</sup> The properties of E33 are  $N_s = 4.0$  sites/nm<sup>2</sup>,  $A_s = 158.1$  m<sup>2</sup>/g,  $C_1 = 1.0$  F/cm<sup>2</sup>,  $C_2 = 0.20$  F/cm<sup>2</sup>, and  $pH_{zpc} = 8.5$  (12). The value of  $\Delta pK_n^0$  is assumed to be the same as for goethite (= 5.6) given by Fukushi and Sverjensky (23). The values of log  $K_1^0$  and log  $K_2^0$  are 5.7 and 11.3, respectively, and the values of log  $K_{Na^+}^0$  and log  $K_{NO_3^-}^0$  are 3.6 and 3.5, respectively (12). The complete list of the ETLM parameters and the relationships among those parameters are presented in Table S1–S4 (SI).

exchange (22). The ETLM parameters used in this prediction are listed in Tables S1–S4 (Supporting Information (SI)).

## Results and Discussion

**Adsorption Isotherms without Buffer.** Arsenate and phosphate adsorption isotherms for E33 at three different pH values (4.0, 7.0, and 10.0) with a solid concentration of 1.0 g/L were obtained without using buffer in our previous study (12). Here, to investigate the dependence of adsorption on solid concentration and to obtain sufficient data at low aqueous equilibrium concentrations, arsenate and phosphate adsorption isotherm tests were conducted at pH 7.0 with a solid concentration of 0.025 g/L. Results are shown in Figure 1 together with the ETLM predictions. No adsorption dependence on solid concentration was observed for either arsenate or phosphate. The ETLM parameters determined in our previous study are listed in Table 1. Although the ETLM overestimated phosphate adsorption at pH 10, the ETLM was generally able to predict arsenate and phosphate adsorption isotherms rather well over a wide range of pH and solute concentrations. At pH 7.0, the ETLM predictions of arsenate and phosphate adsorption isotherms at a solid concentration of 0.025 g/L were identical to those at a solid concentration of 1.0 g/L.

### Modeling Carbonate Adsorption Edge on a Goethite.

Carbonate adsorption on goethite (34) under closed and open system conditions are predicted using the ETLM in

Figure 2. Under most conditions, the ETLM could describe the adsorption data well using the monodentate–mononuclear inner-sphere complex of carbonate ( $>SO-COO^-$ ). Although the discrepancies between the experimental data and the ETLM calculations are larger at higher pH, the standard deviations of the experimental data are also larger at higher pH. The ETLM predictions are mostly within the range of the standard deviations of experimental values.

**Adsorption Isotherms with Buffers.** Arsenate adsorption isotherms conducted by Method 1 are shown in Figure 3. Comparing the adsorption isotherms conducted at pH 7.0 with HEPES and those conducted at pH 7.0 without buffer, no measurable effect of HEPES was observed (Figure 3). However, at lower aqueous equilibrium concentrations of arsenate and phosphate ( $\sim 1.3$   $\mu$ M, 100  $\mu$ g/L as As), the adsorption isotherms measured at pH 7.0 with NaHCO<sub>3</sub> are significantly different from the isotherms without buffer. Conversely, above surface coverage of approximately 1.0–2.0  $\mu$ mol/m<sup>2</sup>, the ETLM systematically underestimated the amount of adsorbed arsenate in the presence of carbonate. This may be due to surface precipitation, surface polymerization, and surface diffusion into the mineral structure. It is somewhat consistent with the results in ref 23 that the ETLM underestimates the amount of adsorbed arsenate at surface coverages above  $\sim 2.5$   $\mu$ mol/m<sup>2</sup>. This can be seen only in the presence of

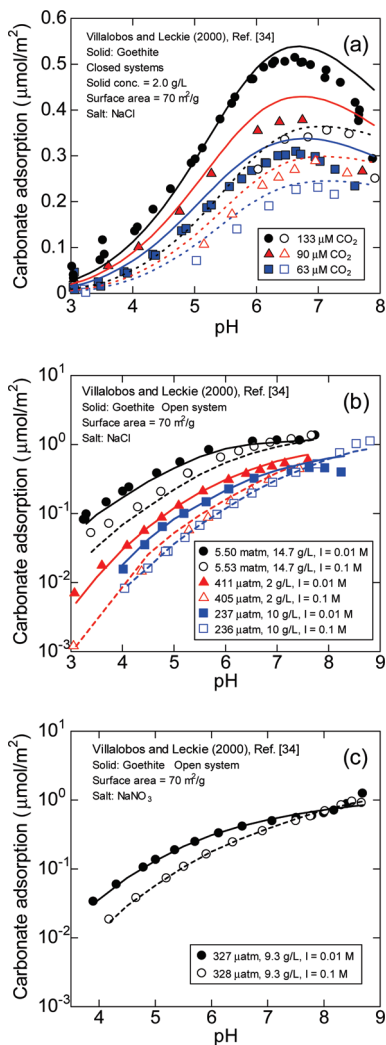


**FIGURE 2.** The ETLM prediction of carbonate adsorption edge on the goethite in a closed system ( $R^2 = 0.96$ ) (a), open system in NaCl solution ( $R^2 = 0.98$ ) (b), and open system in NaNO<sub>3</sub> solution ( $R^2 = 0.99$ ) (c). The data are obtained from the study conducted by Villalobos and Leckie (34). Closed and open symbols indicate 0.01 and 0.1 M background electrolyte solution, respectively.

carbonate, and further research is necessary to understand the mechanism.

The competitive effects of carbonate on arsenate and phosphate adsorption isotherms were predicted using the ETLM as shown in Figure 3. The adsorption equilibrium constant of carbonate for E33 referring to the hypothetical 1.0 M standard state was estimated from the constants for goethite reported by Villalobos (30) listed in Table S5 of the SI using the equations below.

$$\log *K_{>SOCOO}^{\theta} = \log *K_{>SOCOO}^{\theta} + \log \left( \frac{N_s A_s}{N^{\ddagger} A^{\ddagger}} \right) \quad (16)$$

$$\log K_{>SOCOO}^{\theta} = -\log *K_{>SOCOO}^{\theta} - \text{pH}_{\text{ZPC}} + \frac{\Delta p K_n^{\theta}}{2} \quad (17)$$

Considering the values of the surface properties, the adsorption equilibrium constant of carbonate for E33 referring to the hypothetical 1.0 M standard state was estimated to be  $10^{-1.6}$ . This value is used in Figure 3 to predict the effects of carbonate on arsenate and phosphate adsorption isotherms. Figure 3 also includes results of sensitivity analyses

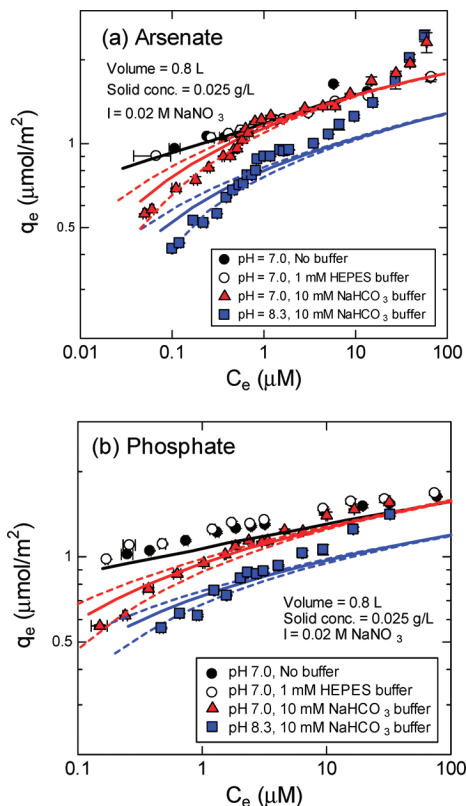


**FIGURE 3.** Arsenate (a) and phosphate (b) adsorption isotherms for E33 at pH 7.0 and 8.3 with buffers (i.e., 1 mM of HEPES and 10 mM of NaHCO<sub>3</sub>) determined by Method 1. Ionic strength in solutions was controlled at 0.02 M using NaNO<sub>3</sub>. Solid lines are the ETLM predictions of adsorption isotherms using the carbonate surface complexation constant predicted by the ETLM theory ( $\log *K_{>SOCOO}^{\theta} = -1.60$ ). Dotted lines are the results of sensitivity analyses for ETLM predictions of adsorption isotherms, and the carbonate surface constants referring to the 1.0 M standard state were adjusted  $\pm 0.25$  (log).

for the adsorption equilibrium constant of carbonate ( $\log K \pm 0.25$ ). The model can describe arsenate and phosphate adsorption isotherms in the presence of carbonate particularly if a small adjustment is made to the predicted equilibrium constant ( $\log K \pm 0.25$ ).

Arsenate adsorption isotherms obtained following Method 2 are shown together with the ETLM predictions in Figure 4, and all adsorption isotherms obtained in this study are shown together in Figure S2 of the SI. No measurable effect of HEPES was observed (Figure 4, Figure S1 of the SI). The arsenate and phosphate adsorption isotherms conducted at pH 7.0 with NaHCO<sub>3</sub> are, however, different from those measured with HEPES at lower arsenate and phosphate aqueous-phase concentrations. In Figure 4, although arsenate adsorption isotherms were described well using the ETLM, the predicted phosphate adsorption isotherms are relatively inaccurate probably due to the inaccurate predictions of phosphate adsorption isotherms in the previous study. Methods 1 and 2 produced different adsorption isotherms when NaHCO<sub>3</sub> was used as a buffer (Figure S2 of the SI) presumably because the ratio of oxyanions/solid in Method 2 is lower than this ratio in Method 1 at the constant NaHCO<sub>3</sub> concentration employed. The error caused by the presence of carbonate during arsenate adsorption isotherm experiments, expressed by  $q_{e(\text{NaHCO}_3)} / q_{e(\text{HEPES})}$ , determined by each of the two experimental methods considered are predicted using the ETLM in Figure 5. This figure shows that carbonate

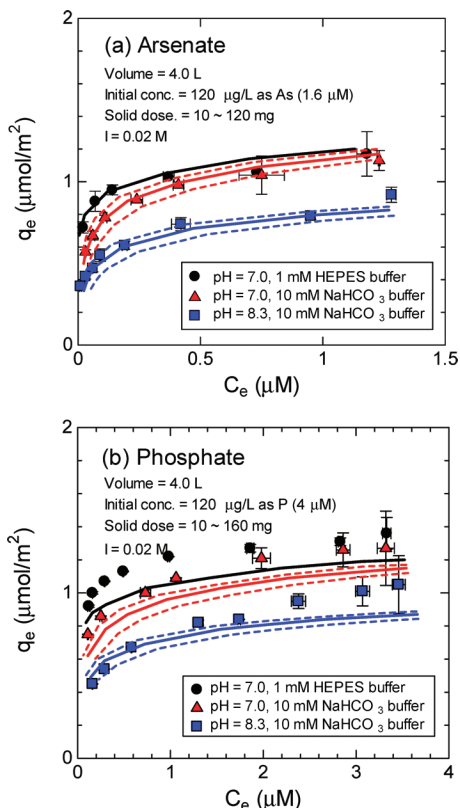


**FIGURE 4.** Arsenate (a) and phosphate (b) adsorption isotherms for E33 at pH 7.0 and 8.3 with buffers (i.e., 1 mM of HEPES and 10 mM of  $\text{NaHCO}_3$ ) determined by Method 2. Ionic strength in solutions was controlled at 0.02 M using  $\text{NaNO}_3$ . Solid lines are the ETLM predictions of adsorption isotherms using the carbonate surface complexation constant predicted by the ETLM theory ( $\log^*K_{\text{CO}_3}^0 = -1.60$ ). Dotted lines are the results of sensitivity analyses for ETLM predictions of adsorption isotherms, and the carbonate surface constants referring to the 1.0 M standard state were adjusted  $\pm 0.25$  (log).

concentrations as low as those typically found in groundwater ( $\sim 10$  mM) can cause significant error in arsenate adsorption isotherms.

**Comparing the Arsenic Adsorptive Capacities of Commercially Major Adsorbents.** Successful ETLM calculation allows quantitative comparison of arsenate adsorption isotherms between E33 and other major commercial adsorbents initially tested under varied experimental conditions in the literature (Figure 6). Arsenate adsorption isotherms determined by Method 1 with organic buffers (5, 6) were compared in Figure 6A, and arsenate adsorption isotherms determined by Method 2 with  $\text{NaHCO}_3$  buffer (7–9) were compared in Figure 6B. Arsenate adsorption isotherms for E33 and an akaganeite ( $\beta\text{-FeOOH}$ ) based wet adsorbent (Granular Ferric Hydroxide, GFH, Siemens) (6, 8) for pH 8.4 cross at an aqueous arsenate concentration of  $\sim 40$   $\mu\text{g/L}$  as As. GFH has a higher adsorptive capacity at concentrations above this threshold (Figure 6A,B). Since adsorptive media shown in Figure 6 are most frequently used in small water systems, this is useful information to choose the best adsorbent for water treatment. In these figures, E33 has higher adsorption capacity than other adsorptive media, which is consistent with the results of extensive pilot tests (3). In the future, newly developed adsorbents should be compared with E33 because of its high adsorptive capacity and the availability of the ETLM parameters.

**Implications.** The results of this study suggest that a typical concentration of carbonate ( $\sim 10$  mM) in groundwater can

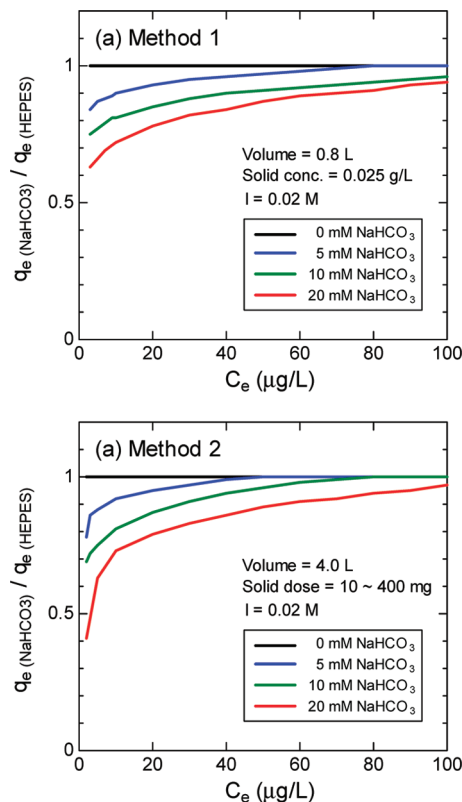


**FIGURE 5.** The ETLM prediction of the equilibrium arsenate adsorption in the presence of carbonate buffer ( $q_{e(\text{NaHCO}_3)}$ ) and in the presence of HEPES ( $q_{e(\text{HEPES})}$ ) as a function of equilibrium aqueous concentration of arsenate illustrating the importance of this effect when studying arsenate adsorption near the U.S. drinking water standard (10  $\mu\text{g/L}$  as As).

compete with arsenate and phosphate for adsorption on a commercial goethite-based adsorbent and play an important role in arsenate mobility especially at arsenate aqueous concentrations below  $\sim 1.3$   $\mu\text{M}$  (100  $\mu\text{g/L}$ ). Although phosphate can compete more strongly with arsenate than carbonate at the same concentration, usually carbonate exists in groundwater at a much higher concentration than phosphate. Moreover, carbonate competition can be a source of uncertainty when arsenate adsorption isotherms are compared at low aqueous arsenate concentration as shown above. The ETLM approach can describe the carbonate competitive effect on arsenate and phosphate adsorption on E33 with the adsorption equilibrium constant of carbonate for E33 estimated from a pure goethite. This implies that adsorption equilibrium constants of other ions for E33 can be obtained from other references using the ETLM approach and that competitive adsorption of arsenate with other ions can be predicted.

## Acknowledgments

This research was supported under Contract No. 06-55254 from the California Department of Public Health, Safe Drinking Water Revolving Fund. The content is solely the responsibility of the authors and does not necessarily represent the official views of the sponsoring organization. Financial support for D. A. Sverjensky and K. Fukushi was provided by a joint NSF-NASA Collaborative Research Grant to the Johns Hopkins University and the Carnegie Institution for Science and DOE Grant DE-FG02-96ER-14616 to Johns Hopkins University. The authors would like to thank the editor and three anonymous reviewers for comments that resulted in significant improvements of this manuscript.

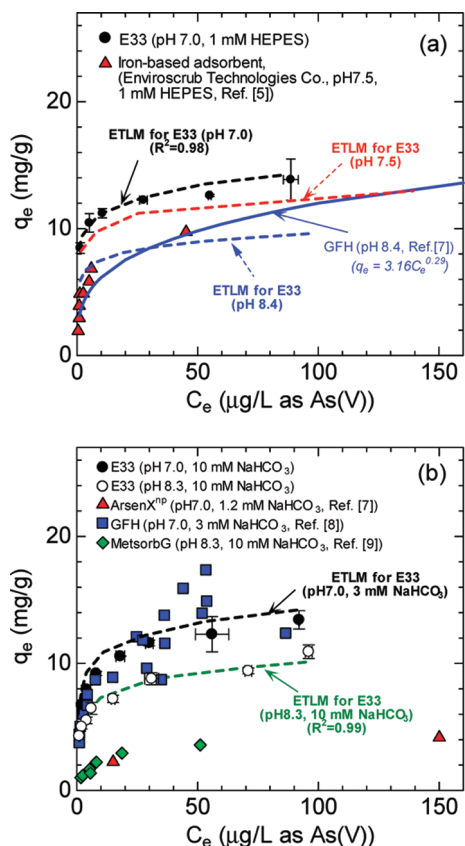


**FIGURE 6.** Comparisons of arsenate adsorption isotherms for various adsorbent media. Arsenate adsorption isotherms determined by Method 1 and using organic buffers were shown and compared in (a), and those determined by Method 2 and using  $\text{NaHCO}_3$  buffer were shown and compared in (b). The solid line in (a) indicate the Freundlich equation obtained for GFH in ref 7. The dotted lines indicate the ETLM simulation results.

### Supporting Information Available

Details on the following: (1) The detailed list of the surface parameters of E33 and the goethite (34) (Table S1); (2) The detailed list of adsorption equilibrium constants of arsenate and phosphate for E33 at different solid concentrations (Table S2, S3); (3) The detailed list of adsorption equilibrium constants of carbonate for E33 and goethite mineral (Table S4); (4) The list of experimental conditions of adsorption isotherms for various adsorbents in the literature (Table S5); (5) The fitted Freundlich curves for arsenate and phosphate adsorption isotherms determined by Method 2 (Figure S1); (6) Comparison of arsenate and phosphate adsorption isotherms determined by Method 1 and 2 (Figure S1). This material is available free of charge via the Internet at <http://pubs.acs.org>.

### Literature Cited

- Nordstrom, D. Public health—Worldwide occurrences of arsenic in ground water. *Science* **2002**, 296 (5576), 2143–2145.
- U.S. Environmental Protection Agency, Arsenic in drinking water. Available at <http://water.epa.gov/lawsregs/rulesregs/sdwa/arsenic/index.cfm>.
- Seigel, M.; Aragon, A.; Zhao, H.; Everett, R.; Aragon, M.; Nocon, M.; Dwyer, B.; Marbury, J.; Kirby, C.; North, K. *Pilot Test of Arsenic Adsorptive Media Treatment Technologies at Socorro Springs*; Sandia National Laboratories: Albuquerque, NM, 2007.
- Dixit, S.; Hering, J. Comparison of arsenic(V) and arsenic(III) sorption onto iron oxide minerals: Implications for arsenic mobility. *Environ. Sci. Technol.* **2003**, 37 (18), 4182–4189.

- Zeng, H.; Arashiro, M.; Giammar, D. E. Effects of water chemistry and flow rate on arsenate removal by adsorption to an iron oxide-based sorbent. *Water Res.* **2008**, 42 (18), 4629–4636.
- Sperlich, A.; Schimmelpfennig, S.; Baumgarten, B.; Genz, A.; Amy, G.; Worch, E.; Jekel, M. Predicting anion breakthrough in granular ferric hydroxide (GFH) adsorption filters. *Water Res.* **2008**, 42 (8–9), 2073–2082.
- Moller, T.; Sylvester, P. Effect of silica and pH on arsenic uptake by resin/iron oxide hybrid media. *Water Res.* **2008**, 42 (6–7), 1760–1766.
- Badruzzaman, M.; Westerhoff, P.; Knappe, D. Intraparticle diffusion and adsorption of arsenate onto granular ferric hydroxide (GFH). *Water Res.* **2004**, 38 (18), 4002–4012.
- Hristovski, K.; Baumgardner, A.; Westerhoff, P. Selecting metal oxide nanomaterials for arsenic removal in fixed bed columns: From nanopowders to aggregated nanoparticle media. *J. Hazard. Mater.* **2007**, 147 (1–2), 265–274.
- Hristovski, K. D.; Westerhoff, P. K.; Crittenden, J. C.; Olsow, L. W. Arsenate removal by nanostructured  $\text{ZrO}_2$  spheres. *Environ. Sci. Technol.* **2008**, 42 (10), 3786–3790.
- Crittenden, J.; Montgomery Watson Harza (Firm), *Water Treatment Principles and Design*, 2nd ed.; John Wiley: Hoboken, NJ, 2005; p 1948.
- Kanematsu, M.; Young, T. M.; Fukushi, K.; Green, P. G.; Darby, J. L. Extended triple layer modeling of arsenate and phosphate adsorption on a goethite-based granular porous adsorbent. *Environ. Sci. Technol.* **2010**, 44 (9), 3388–3394.
- Antelo, J.; Avena, M.; Fiol, S.; Lopez, R.; Arce, F. Effects of pH and ionic strength on the adsorption of phosphate and arsenate at the goethite–water interface. *J. Colloid Interface Sci.* **2005**, 285 (2), 476–486.
- AWWA Research Foundation. *Adsorbent Treatment Technologies for Arsenic Removal*; AWWA: 2005.
- Meng, X.; Bang, S.; Korfiatis, G. Effects of silicate, sulfate, and carbonate on arsenic removal by ferric chloride. *Water Res.* **2000**, 34 (4), 1255–1261.
- Good, N. E.; Winget, G. D.; Winter, W.; Connolly, T. N.; Izawa, S.; Singh, R. M. M. Hydrogen ion buffers for biological research. *Biochemistry* **1966**, 5 (2), 467–477.
- Stachowicz, M.; Hiemstra, T.; Van Riemsdijk, W. Arsenic-bicarbonate interaction on goethite particles. *Environ. Sci. Technol.* **2007**, 41 (16), 5620–5625.
- Rahnemaie, R.; Hiemstra, T.; van Riemsdijk, W. Carbonate adsorption on goethite in competition with phosphate. *J. Colloid Interface Sci.* **2007**, 315 (2), 415–425.
- Arai, Y.; Sparks, D.; Davis, J. Effects of dissolved carbonate on arsenate adsorption and surface speciation at the hematite–water interface. *Environ. Sci. Technol.* **2004**, 38 (3), 817–824.
- Schwertmann, U.; Cornell, R. M. *Iron Oxides in the Laboratory: Preparation and Characterization*, 2nd completely rev. and extended ed.; Wiley-VCH: Weinheim; New York, 2000; p xviii, 188.
- AdEdge Technologies Inc. <http://www.adedgetechnologies.com/index.html>.
- Sverjensky, D. A.; Fukushi, K. Anion adsorption on oxide surfaces: Inclusion of the water dipole in modeling the electrostatics of ligand exchange. *Environ. Sci. Technol.* **2006**, 40 (1), 263–271.
- Fukushi, K.; Sverjensky, D. A. A predictive model (ETLM) for arsenate adsorption and surface speciation on oxides consistent with spectroscopic and theoretical molecular evidence. *Geochim. Cosmochim. Acta* **2007**, 71 (15), 3717–3745.
- Sahai, N.; Sverjensky, D. GEOSURF: A computer program for modeling adsorption on mineral surfaces from aqueous solution. *Comput. Geosci.* **1998**, 24 (9), 853–873.
- Loring, J.; Sandstrom, M.; Noren, K.; Persson, P. Rethinking Arsenate Coordination at the Surface of Goethite. *Chem.—Eur. J.* **2009**, 15 (20), 5063–5072.
- Salazar-Camacho, C.; Villalobos, M., III. Unifying arsenate adsorption behavior through a variable crystal face—Site density model. *Geochim. Cosmochim. Acta* **2010**, 74 (8), 2257–2280.
- Sverjensky, D. A. Standard states for the activities of mineral surface sites and species. *Geochim. Cosmochim. Acta* **2003**, 67 (1), 17–28.
- Sverjensky, D. Prediction of surface charge on oxides in salt solutions: Revisions for 1: 1 (M+L<sup>-</sup>) electrolytes. *Geochim. Cosmochim. Acta* **2005**, 69 (2), 225–257.
- Ostergren, J. D.; Trainor, T. P.; Bargar, J. R.; Brown, G. E.; Parks, G. A. Inorganic ligand effects on Pb(II) sorption to goethite ( $\alpha$ -

- FeOOH) - I. Carbonate. *J. Colloid Interface Sci.* **2000**, 225 (2), 466–482.
- (30) Villalobos, M.; Leckie, J. Surface complexation modeling and FTIR study of carbonate adsorption to goethite. *J. Colloid Interface Sci.* **2001**, 235 (1), 15–32.
- (31) Wijnja, H.; Schulthess, C. P.; Carbonate adsorption mechanism on goethite studied with ATR-FTIR, DRIFT, and proton coadsorption measurements. *Soil Science Society of America Journal* **2001**, 65 (2), 324–330.
- (32) Bargar, J. R.; Reitmeyer, R.; Davis, J. A. Spectroscopic confirmation of uranium(VI)-carbonate adsorption complexes on hematite. *Environ. Sci. Technol.* **1999**, 33 (14), 2481–2484.
- (33) Bargar, J. R.; Kubicki, J. D.; Reitmeyer, R.; Davis, J. A. ATR-FTIR spectroscopic characterization of coexisting carbonate surface complexes on hematite. *Geochim. Cosmochim. Acta* **2005**, 69, 1527–1542.
- (34) Villalobos, M.; Leckie, J. Carbonate adsorption on goethite under closed and open CO<sub>2</sub> conditions. *Geochim. Cosmochim. Acta* **2000**, 64 (22), 3787–3802.
- (35) Hiemstra, T.; Rahnemaie, R.; van Riemsdijk, W. H. Surface complexation of carbonate on goethite: IR spectroscopy, structure and charge distribution. *J. Colloid Interface Sci.* **2004**, 278 (2), 282–290.

ES1026745